

Tensile and Thermal Properties of Poly(lactic acid)/Egg Shell Powder Composite Films

B. Ashok ¹, S. Naresh ², K. Obi Reddy ³, K. Madhukar ¹, J. Cai ⁴, L. Zhang ⁴, A. Varada Rajulu ²

¹ Department of Physics, Osmania University, Hyderabad – 500007, India.

² Department of Polymer Science and Technology, Sri Krishnadevaraya University, Anantapur-515003, India.

³ Department of Chemical Engineering Technology, Doornfontein Campus, P.O. Box 17011, University of Johannesburg, Johannesburg-2028, South Africa

⁴ Department of Chemistry, Wuhan University, Wuhan-5430072, P. R. China

Abstract

Biodegradable composite films of Poly(lactic acid)(PLA)/Egg shell powder (ESP) were prepared by film casting method using chloroform as the solvent. ESP was loaded in PLA in 1 to 5 wt.%. The films were subjected to tensile, FTIR spectral, thermogravimetric, X-ray and microscopic analyses. The tensile strength and modulus of the composite films were found to be higher than PLA and increased with ESP content upto 4 wt.% and then decreased. A reverse trend was observed in the case of %elongation at break. The X-ray spectra of the composites indicated increase in crystallinity with ESP content. The optical micrographs indicated uniform distribution of ESP particles in the composite films. However, the fractographs indicated agglomeration of ESP particles at 5 wt.% loading. The FTIR spectra revealed no specific interactions between PLA and ESP. The thermal stability of the composite films increased with ESP content.

Keywords: Poly(lactic acid); Egg shell powder; tensile properties; thermal stability; X-ray diffraction.

***Corresponding author:** K. Obi Reddy

Department of Chemical Engineering Technology, Doornfontein Campus, P.O. Box 17011, University of Johannesburg, Johannesburg-2028, South Africa

Tel.: +27 84660 6269; E-mail address: obireddyk80@gmail.com & obik@uj.ac.za

Introduction

Environmental concerns and sustainability issues related with petrochemical-based polymers have motivated considerable engineering and scientific efforts devoted to the discovery, development, and modifications of biodegradable and renewably-derived polymers over the past several decades [1-2]. The selection of biodegradable polymers offers the possibility of obtaining innovative types of eco-friendly and fully degradable composites with an extensive application potential in several advanced technological sectors [3]. In recent years, there is great interest in biodegradable polymers obtained from renewable resources, such as starch, poly(lactic acid), polycaprolactone, polyhydroxybutyrate and poly(butylene adipate-co-terephthalate) that are notable for their ability to maintain the biodegradability of the final product [4]. One conventional such polymer is poly(lactic acid) or poly(lactide) (PLA), which is the first commodity plastic produced from annually renewable resources. PLA is recyclable, biodegradable, thermoplastic, aliphatic linear polyester derived from renewable resources such as corn starch, potatoes, sugarcane or other biomasses [5]. These beneficial properties generally enable PLA to compete with petroleum-based plastics in many application areas and also it is biocompatible with non-toxic degradation products (at low concentrations), making it a natural choice for many biomedical applications [6, 7]. However, the drawbacks of high price, sensitivity to water, fast physical aging, inherent brittleness, limited impact resistance and large stiffness and slow crystallization rate restrict the industrial applicability of PLA [8-10]. As a conclusion result, PLA is tailored in many ways to develop materials with suitable property profiles, among others by plasticization, impact modification and by the introduction of fillers or fibers, particularly for structural applications [11-18].

A preferred solution referring to blending PLA with low-cost renewable fillers and bio-based toughening agents is mainly considered in producing environment-friendly composite materials with superior properties. Chicken egg shell powder (ESP) as an important renewable filler of PLA attracts great attention because of its low price and easy availability. Chicken eggshell is a poultry industrial byproduct that has been listed worldwide as one of the worst environmental problems, especially in those countries where the egg product industry is well developed [19]. Eggshell contains about 95 % calcium carbonate in the form of calcite and remaining organic materials such as type X collagen, sulfated polysaccharides and other proteins [19]. Although

there have been several attempts to use eggshell components for different applications, its chemical composition and availability makes eggshell a potential source of filler in polymer composites [19-21]. Biocomposites that consist of natural polymers and inorganic particles have gained more interest as environmentally friendly and biofunctional materials due to their interesting properties such as biocompatibility, biodegradability and potential applications in industrial fields.

The objective of this work was to improve the properties of PLA, reduce its cost by using low cost bio filler and add value to the waste filler. With our best knowledge, no direct reference has suggested an effective methodology for strength improvement of PLA/egg shell powder composite via simple solvent film casting method. In the present work, the authors used PLA as matrix and loaded it with 1 to 5 wt.% of egg shell powder (ESP) and studied the effect of ESP loadings on the tensile properties, thermal stability and crystallinity of PLA/ESP composites. Scanning electron microscope and FTIR studies were carried out to provide an insight into the fiber-matrix adhesion and interactions.

Materials and methods

Materials

PLA [$M_w=1.3 \times 10^5$, (M_w/M_n) = 1.9] was supplied by Zhejiang Hisun chemical company limited, China. The supplier indicated L- and D- isomer contents of PLA as 94% and 6% respectively. Waste hen egg shells were washed thoroughly in water and dried in the open for several days. The cleaned and dried egg shells were made into fine powder using a kitchen grinder-mixer and sieved. The ESP which passed through 25 μm sieve was used as the filler after drying. Chloroform (Analytical grade) supplied by S.D. fine chemicals (Mumbai, India) was used as received.

Preparation of PLA/ESP composite films

PLA was dissolved in chloroform to make 10 wt.% solution. Dried ESP was added to this solution in 1 to 5 wt.% and stirred well with mechanical stirrer. The films of PLA and PLA/ESP composites were made by film casting method.

Microscopic analysis

Optical micrographs of the surface of PLA/ESP composites were recorded using a Leica DMLP polarized optical microscope. The fractographs of the brittle fractured and gold sputtered composite films were recorded using a JSM 6700 F scanning electron microscope.

Tensile testing

Rectangular film strips of 100 mm X 10 mm dimensions with 50 μm thickness were tested for tensile properties using an Instron 3365 Universal testing machine maintaining a gauge length of 50mm at a strain rate of 100 mm min^{-1} . For each set, ten specimens were tested and the average values reported.

FTIR spectral analysis

The FTIR spectra of PLA, ESP and PLA/ESP composite films were recorded in the wavenumber range of 4000 to 600 cm^{-1} using an Analect RTF-65A spectrometer in the reflection mode.

X-ray diffraction analysis

The wide angle X-ray diffractograms of PLA, ESP and PLA/ESP composite films were recorded on a Rigaku Ultima IV X-ray diffractometer. The system has a rotating anode generator with copper target and a wide angle goniometer. The generator was operated at 40 kV and 30 mA and the samples were scanned in the 2θ range of 5 to 80°.

Thermogravimetric analysis

Primary thermograms of PLA and PLA/ESP composite films were recorded using a thermogravimetric analyzer (Perkin Elmer TGA-7). Samples with approximately 10 mg weight were loaded in platinum pans and heated from 30 to 600 $^{\circ}\text{C}$ at a heating rate of 10 $^{\circ}\text{C min}^{-1}$ under nitrogen dynamic flow (100 mL min^{-1}).

Results and Discussion

The films produced from PLA had good processability during solvent casting method. The PLA films showed good flexibility and without apparent cracks. The egg shell powder reinforced PLA composite films were homogeneously overlaid the surfaces without changing the appearance of the sheets, and its presence did not change the thickness appreciably, which was around 50 μm .

In order to assess the uniform dispersion of ESP particles in PLA matrix, the optical micrographs of the composites were recorded and are presented in Figure 1. It is evident from Fig.1 that the ESP particles were dispersed uniformly in the composites (ESP particles are indicated by arrows). Both physical and chemical interactions may be responsible for such uniform dispersion.

In order to assess the mechanical performance of PLA/ESP composite films, their tensile properties were studied. Figure 2 shows the stress-strain curves of PLA and PLA/ESP composite films. The effect of filler loading on the tensile (strength, modulus and elongation at break) properties of ESP filled PLA composite films were presented in Table 1. From Table 1, it can be observed that the tensile strength and modulus increased with filler content up to 4 wt.% filler loading and decreased thereafter. This discontinuity could be attributed to increased filler quantity leading to weaker filler-matrix interface and agglomeration of filler particles, which consequently decreases the strength and modulus. This is probably because of a better interfacial adhesion between the filler and the matrix by the Van der Waals or induction interactions. However, in all the cases, the tensile strength and modulus of the composite films were found to be higher than that for the matrix. At the composition of 4 wt.% filler by weight, tensile strength and modulus of the composite films were found to be 30.6 MPa and 1964 MPa respectively. The increase in tensile strength and modulus of composite films, over the matrix were as follows 82.1 and 70.4% respectively. However, from Table 1, it can be observed that the % elongation at the break decreased with increasing filler loading. Increased filler loading in the matrix resulted in the stiffening and hardening of the composite films and the recipe took away shape ductile.

The observation of the morphology of composite films was performed by scanning electron microscopy. Figure 3 shows the micrographs of the brittle fractured composite films with different filler loadings. From Figure 3 (a-d), it is evident that ESP particles were distributed uniformly and individually in the PLA/ESP composites with 1 to 4 wt.% ESP content. However, from Figure 3(e), it can be observed that the ESP particles were agglomerated at some places when the ESP content was 5 wt.%. Further, voids are not appearing in the composites because solvent completely evaporated in the composites during the film casting. Also no gaps appeared between the ESP and PLA due to the hydrophilic behavior of filler and matrix.

In order to further investigate the interactions between ESP and PLA in the PLA/ESP composites FTIR spectra were recorded. Figure 4 presents the FTIR spectra of PLA, ESP and PLA/ESP composites. From Fig.4, it is evident that neat PLA shows the absorption bands at 3659 cm^{-1} corresponding to the terminal OH group. The other bands at 2994 and 2946 cm^{-1} were assigned to the $-\text{CH}$ asymmetric and symmetric stretching vibrations respectively of $-\text{CH}_3$ groups in the side chains. The band at 1454 cm^{-1} was assigned to the bending vibration of $-\text{CH}$. A strong absorption band at 1743 cm^{-1} was assigned to the stretching vibration of carbonyl ($-\text{C}=\text{O}$) groups from the repeated ester units [22]. Another strong absorption band at 1182 cm^{-1} was assigned to stretching vibration of $-\text{C}-\text{O}$ in $-\text{CH}-\text{O}$ of polymer chains. The rocking triplet peaks at 1130 , 1082 and 1038 cm^{-1} correspond to C-O stretching vibrations in $-\text{CO}-\text{O}$ groups [6]. The absorption bands at 956 and 870 cm^{-1} were assigned to C-C stretching of the single bond. A strong absorption band at 749 cm^{-1} was assigned to the deformation vibration of $-\text{CH}_3$ groups. The FTIR spectrum of ESP revealed major absorption bands at 1415 , 879 and 700 cm^{-1} which were assigned to asymmetric stretching, out of plane bending and in-plane bending vibration modes respectively of $(\text{CO}_3)^{2-}$ molecules [23, 24]. Also a broad band of low intensity in the range of $3700-3060\text{ cm}^{-1}$ was attributed to traces of water together with very weak broad band around 1650 cm^{-1} to hydroxyl groups (probably from carboxylic acid group of minor constituent protein) [23]. From Figure 4, it is also evident that the spectra of PLA/ESP are similar to the spectrum of PLA indicating predominantly physical interactions without the formation of new functional groups. However, the intensity of the band at 1743 cm^{-1} was found to be higher than that of PLA. Further, in the $1266-1038\text{ cm}^{-1}$ range, the C-O stretching bands of composites were slightly more intense due to the hydrogen bonds between the C-O of PLA and O-H groups of ESP filler.

As ESP is crystalline due to its CaCO_3 major content, it is worthwhile to investigate the effect of ESP on the crystallinity of PLA/ESP composites. The X-ray diffractograms of ESP, PLA and PLA/ESP composites are presented in Fig.5. From Figure 5, it is evident that for ESP, a main sharp peak at $2\theta \sim 29^\circ$ appeared resulting from (211) plane of CaCO_3 [25]. As PLA is amorphous, no peaks in the region of interest were observed. Because of overlapping of ESP and the amorphous PLA halo, the peaks of PLA/ESP composites could not be identified correctly. In order to overcome this problem, the X-ray diffractograms of PLA/ESP composites were highlighted in the $2\theta = 29.2^\circ$ to 30.6° region and are presented in Figure 6. From Figure 6, the

crystalline peaks corresponding to ESP in the PLA/ESP composites can be observed in and around 29.8°. Thus the induced crystallinity by ESP in PLA/ESP composites may also be responsible for their increased tensile properties.

In order to study the effect of ESP on the thermal stability of PLA/ESP composites, the thermogravimetric analysis was carried out. Figure 7 presents the primary thermograms of PLA and PLA/ESP composites. It is evident from Figure 7 that the thermal stability of the PLA/ESP composites was higher than that of PLA and increased with ESP content. Further, the char content of the composites was also higher than for PLA. This as per expectation as ESP due to its major component of crystalline CaCO₃ has higher thermal stability than the amorphous PLA.

Conclusion

Using chloroform as the solvent, PLA and PLA/ESP composite films with 1 to 5 wt.% ESP were prepared by solution casting technique. The effect of ESP on the tensile properties, crystallinity and thermal stability of the composites was studied. The tensile strength and modulus of the composites was found to be higher than those of the matrix and increased with ESP content upto 4 wt.% and then decreased. The % elongation at break showed a reverse trend. Though the optical micrographs showed uniform distribution of ESP in the composites for all concentrations, the fractographs indicated agglomeration of ESP particles for a loading of 5 wt.%. The X-ray diffractograms indicated induced crystallinity in the composites by ESP. The FTIR spectra did not reveal any appreciable specific interactions between PLA and ESP. The thermal stability of the composites was found to be higher than PLA. Thus ESP improved the properties of PLA. This process reported here opens a new aperture to the high value-added applications of egg shell powder.

Acknowledgements

One of the authors (AVR) thanks the Council of Scientific and Industrial Research (CSIR) of India for the award of an Emeritus Scientist Scheme [21(o842) 11/EMR II dt: 10-05-2011].

Reference

1. Zhang, L., C. Xiong, and X. Deng. 1995. Biodegradable polyester blends for biomedical application. *J. Appl. Polym. Sci.* 56 (4):103-112.
2. Sinclair, R. G. 1996. The case for polylactic acid as a commodity packaging plastic. *J. Macromol. Sci. Part A.* 33(5): 585-597.
3. Thakur, V.K., A.S. Singha and M.K. Thakur. 2012. Green composites from natural fibers: Mechanical and chemical aging properties. *Int. J. Polym. Anal. Charact.* 17(6): 401-407.
4. Lim, L. T., R. Auras, and M. Rubino. 2008. Processing technologies for poly(lactic acid). *Prog. Polym. Sci.* 33(8): 820-852.
5. Hashima, K., S. Nishitsuji, and T. Inoue. 2010. Structure-properties of super-tough PLA alloy with excellent heat resistance. *Polymer* 51(17): 3934–3939.
6. Auras, R., B. Harte, and S. Selke. 2004. An overview of polylactides as packaging materials. *Macromol. Biosci.* 4(9): 835-864.
7. Feng, S. S., L. Mu, K. Y. Win, and G. Huang. 2004. Nanoparticles of biodegradable polymers for clinical administration of paclitaxel. *Current Medicinal Chemistry* 11(4): 413-424.
8. Martin, O., and L. Averous. 2001. Poly(lactic acid): plasticization and properties of biodegradable multiphase systems. *Polymer* 42(14): 6209-6219.
9. Tang, Z. B., C. Z. Zhang, X. Q. Liu, and J. Zhu. 2012. The crystallization behavior and mechanical properties of polylactic acid in the presence of a crystal nucleating agent. *J. Appl. Polym. Sci.* 125(2): 1108-1115.
10. Wang, T., Y. Yang, C. Z. Zhang, Z. B. Tang, H. N. Na, and J. Zhu. 2013. Effect of 1,3,5-trialkyl-benzenetricarboxylamide on the crystallization of poly(lactic acid). *J. Appl. Polym. Sci.* 130(2): 1328-1336.
11. Ljungberg, N., and B. Wesslen. 2003. Tributyl citrate oligomers as plasticizers for poly(lactic acid): thermo-mechanical film properties and aging. *Polymer* 44(25):7679–7688.
12. Afrifah, K. A., and L. M. Matuana. 2010. Impact modification of polylactide with a biodegradable ethylene/acrylate copolymer. *Macromol. Mater. Eng.* 295(9):802–811.
13. Anderson, K. S., K. M. Schreck, and M. A. Hillmyer. 2008. Toughening polylactide. *Polym. Rev.* 48(1):85–108.
14. Ganster, J., and H-P. Fink. 2010. PLA-based bio- and nanocomposites. In: Lau AK-T, Hussain F, Lafdi K, editors. *Nano- and biocomposites*. Boca Raton: CRC press, p.p. 275–90.

15. Darie, R. N., R. Bodirlau, C. A. Teaca, J. Macyszyn, M. Kozlowski and I. Spiridon. 2013. Influence of accelerated weathering on the properties of polypropylene/polylactic acid/eucalyptus wood composites. *Int. J. Polym. Anal. Charact.* 18(4): 315-327.
16. V. Sedlarik, N. Saha, I. Kuritka & P. Saha. 2006. Preparation and characterization of poly (vinyl alcohol)/lactic acid compounded polymeric films. *Int. J. Polym. Anal. Charact.* 11(4): 253-270.
17. H. Balakrishnan, A. Hassan, M. Imran & M. U. Wahit. 2012. Toughening of polylactic acid nanocomposites: A short review. *Polym. Plast. Technol. Eng.* 51(2): 175-192.
18. Y. Tajitsu, M. Kanesaki, M. Tsukiji, K. Imoto, M. Date & E. Fukada. 2005. Novel tweezers for biological cells using piezoelectric polylactic acid fibers. *Ferroelectrics* 320(1), 133-139.
19. Hassan, S. B., V. S. Aigbodion, and S. N. 2012. Patrick. Development of polyester/eggshell particulate composites. *Tribology in Industry* 34(4): 217-225.
20. Patricio, T., Q. Raul, M. Y. Pedram, and L. A. Jose. 2007. Eggshell, a new bio-filler for polypropylene composites. *Mater. Lett.* 61(22): 4347-4350.
21. Hussein, A. A., R. D. Salim, and A. A. Sultan. 2011. Water absorption and mechanical properties of high – density polyethylene/egg shell composite. *Journal of Basrah Researches (Sciences)*, 37(3A) 36-42.
22. Wang, N., X. Zhang, X. Ma, and T. Fang. 2008. Influence of carbon black on the properties Of plasticized poly(lactic acid) composites. *Polym. Degrad. Stabil.* 93(6): 1044-1052.
23. Engn, B., H. Demirtas, and M. Eken. 2006. Tmperature effects on egg shells investigated by XRD, IR and ESR techniques. *Radia. Phy. Chem.* 75(2): 268-277.
24. Gergley, G., F. Weber, I. Lukacs, A. L. Toth, Z. E. Horvath, J. Mihaly, and C. Balazsi. 2010. Preparation and characterization of hydroxyapatite from egg shell. *Ceramics International* 36(2): 803-806.
25. Gunasekhar, K., and T. P. Sastry. 2011. Preparation and characterization of novel bone graft composites containing bone ash and egg shell powder. *Bulletin of Materials Science* 34(1): 177-181.

Caption for Figures

Figure 1. Optical micrographs of PLA/ESP composites with ESP content of (a) 1 wt.%; (b) 2 wt.%; (c) 3 wt.%; (d) 4 wt.% and (e) 5 wt.%

Figure 2. Stress-Strain curves of PLA and PLA/ESP composites with 1 to 5 wt.% ESP

Figure 3. Fractographs of PLA/ESP composites with ESP content of (a) 1 wt.%; (b) 2 wt.%; (c) 3 wt.%; (d) 4 wt.% and (e) 5 wt.%.

Figure 4. FTIR spectra of PLA, ESP and PLA/ESP composites

Figure 5. X-ray diffractograms of PLA, ESP and PLA/ESP composite films

Figure 6. X-ray diffractograms of PLA/ESP composite films in a narrow 2θ range.

Figure 7. Primary thermograms of PLA and PLA/ESP composites with 1 to 5 wt.% ESP.

Caption for Table

Table 1. Tensile properties of Egg shell powder reinforced PLA composites as a function of Egg shell powder content

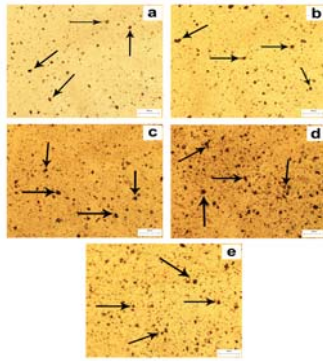


Figure1. Optical micrographs of PLA/ESP composites with ESP content of (a) 1 wt.%; (b) 2 wt.%; (c) 3 wt.%; (d) 4 wt.% and (e) 5 wt.%

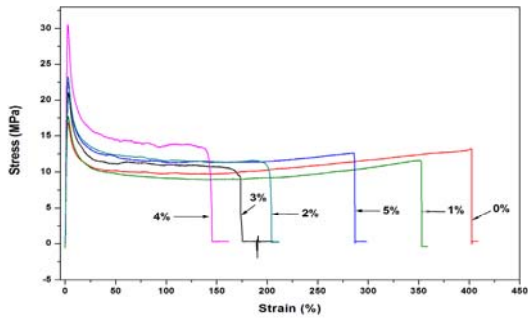


Figure 2. Stress-Strain curves of PLA and PLA/ESP composites with 1 to 5 wt.% ESP

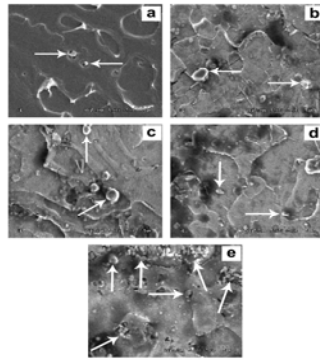


Figure 3. Fractographs of PLA/ESP composites with ESP content of (a) 1 wt.%; (b) 2 wt.%; (c) 3 wt.%; (d) 4 wt.% and (e) 5 wt.%.

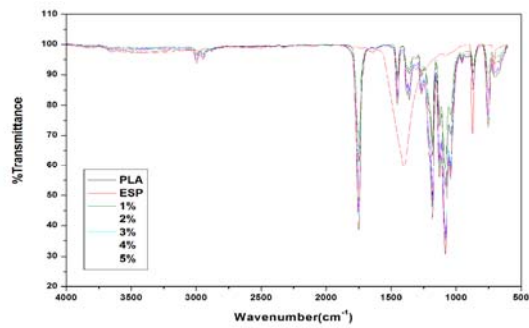


Figure 4. FTIR spectra of PLA, ESP and PLA/ESP composites

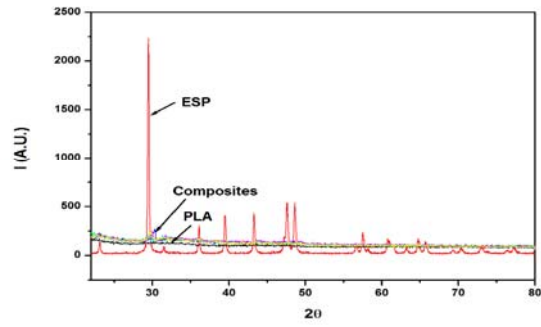


Figure 5. X-ray diffractograms of PLA, ESP and PLA/ESP composite films

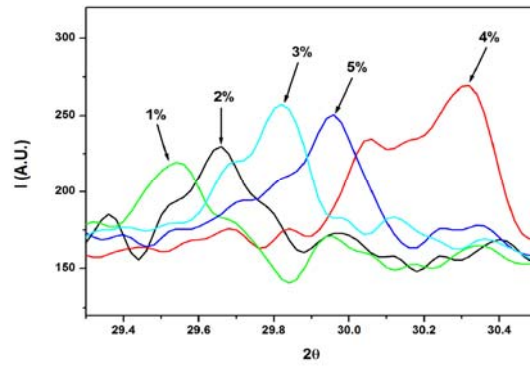


Figure 6. X-ray diffractograms of PLA/ESP composite films in a narrow 2θ range.

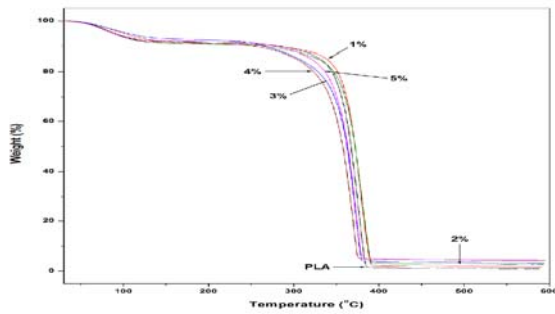


Figure 7. Primary thermograms of PLA and PLA/ESP composites with 1 to 5 wt.% ESP.

Table 1. Tensile properties of Egg shell powder reinforced PLA composites as a function of Egg shell powder content

Wt.% ESP in the composite	Maximum Stress (MPa)	Young's Modulus (MPa)	Elongation at Break (%)
0	16.8±0.5	1152±32	402±27
1	17.7±0.4	1171±51	352±19
2	21.1±0.8	1433±69	213±25
3	25.5±1.1	1767±66	173±23
4	30.6±1.7	1964±126	143±16
5	22.5±0.9	1389±95	286±35